

Supporting Information for “Disentangling Global Warming, Multidecadal Variability, and El Niño in Pacific Temperatures”

Robert C. Wills¹, Tapio Schneider², John M. Wallace¹, David S. Battisti¹,

Dennis L. Hartmann¹,

Contents of this file

1. Text S1
2. Table S1
3. Figures S1 to S7

Text S1

Table S1 shows the properties of the EOFs, LFCs, and other indices of Pacific SST variability.

¹Department of Atmospheric Sciences,
University of Washington, Seattle, WA

²Environmental Science and Engineering,
California Institute of Technology,
Pasadena, CA

Fig. S1 shows the leading 3 EOFs of Pacific SST (Table S1 shows properties of these EOFs), illustrating mode mixing between global warming, ENSO, and the PDO. The warming trend is split between EOFs 1 and 2. The correlations of the principal components of EOFs 1-3 with PDO* and ENSO* shows that all 3 EOFs contain large components of PDO and ENSO. These 3 EOFs are transformed using LFCA to obtain the LFCs in Fig. 1, including the PDO* and ENSO* indices.

Fig. S2 shows the regressions of 20th Century Reanalysis sea-level pressure [*Compo et al.*, 2011] on indices discussed in the main text. LFCs are those in Fig. 1, based on LFCA of the first 3 EOFs of Pacific SST using a 10-year lowpass filter.

Fig. S3 shows a side-by-side comparison of the traditional PDO and the PDO-like mode (LFP/LFC 4) of the 30 EOF analysis. Also shown is the regression of Pacific SSTs onto the difference between the PDO index and LFC 4 (scaled by its correlation with the PDO index). This highlights the region where these definitions of PDO differ.

Fig. S4 shows the PDO-like mode in 4 tests of the sensitivity to the LFCA parameters: EOF truncation number and lowpass cutoff timescale.

Fig. S5 illustrates the extent to which the PDO regression pattern depends on subtle details of the PDO index. It shows a PDO-like mode obtained through transformation of the first 3 EOFs of Pacific SST based on maximization of the ratio of 3-yr variance (using successive 3-yr highpass and 3-yr lowpass filters) to total variance. The first mode from this rotation is related to ENSO, and is not shown. The second-mode is similar to the PDO (Fig. S5b), but has a much weaker relationship with tropical SSTs, especially when compared to the *Mantua et al.* [1997] PDO definition (Fig. S5a). A side-by-side

comparison of the two indices (Fig. S5c) shows that the indices are almost identical, except in big El Niño years (primarily 1982/83 and 1997/98). They have an 86% correlation overall. The regression of the difference between these indices on global SSTs primarily shows anomalies in the eastern equatorial Pacific (Fig. S5d). This provides a cautionary tale in the interpretation of such SST regression maps. The tropical component of the traditional PDO comes not from its decadal variability, but from averaging in the effects of a few large El Niño years.

Fig. S6 shows the coherence spectra of PDO-like modes discussed in the main text and the traditional *Mantua et al.* [1997] PDO index.

Fig. S7 provides an illustration of the sensitivity of the PDO-like mode in Fig. 4d to the LFCA parameters. Once 20 EOFs are included, LFCA converges on a representation of the PDO that does not exhibit a lot of sensitivity to parameters (assuming the lowpass cutoff is greater than 6 years).

Table 1. Properties of the EOFs, LFCs, and other indices of Pacific SST variability. Here, LFCs are those shown in Fig. 1, PacMean is the Pacific-basin mean, and PDO is based on the traditional PDO definition [*Mantua et al.*, 1997]. The ratio of low-frequency to total variance r is based on a 10-year lowpass filter. The domain mean is computed over the full Pacific basin (45°S-70°N). The trend is assessed from linear regression over the full time period and given in standard deviations per century.

	r	Domain mean (°C)	Trend in σ per century	Correlation with PDO*	Correlation with ENSO*
PC 1	0.33	0.20	1.3	53%	68%
PC 2	0.67	0.18	2.3	-34%	-38%
PC 3	0.20	0.01	0.05	78%	-62%
LFC 1	0.84	0.26	2.6	0	0
LFC 2	0.29	0.05	-0.05	100%	0
LFC 3	0.06	0.07	-0.02	0	100%
PacMean	0.78	0.24	2.5	18%	23%
PDO	0.27	0.05	0.21	94%	14%
Niño3.4	0.09	0.06	0	44%	83%

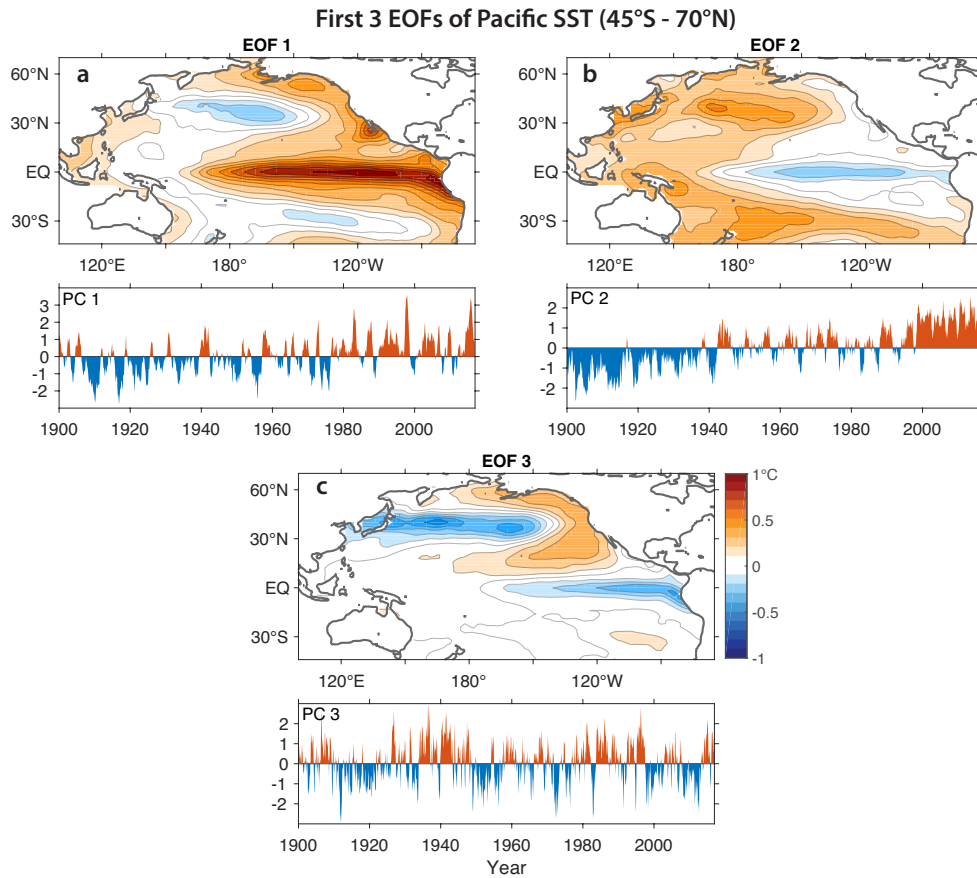


Figure S1. First 3 EOFs of Pacific SST illustrate mode mixing before application of LFCA. (a)-(c) EOFs 1-3 of Pacific SST and the corresponding principal components. All 3 EOFs show a mix of ENSO, PDO, and global warming (see Table 1).

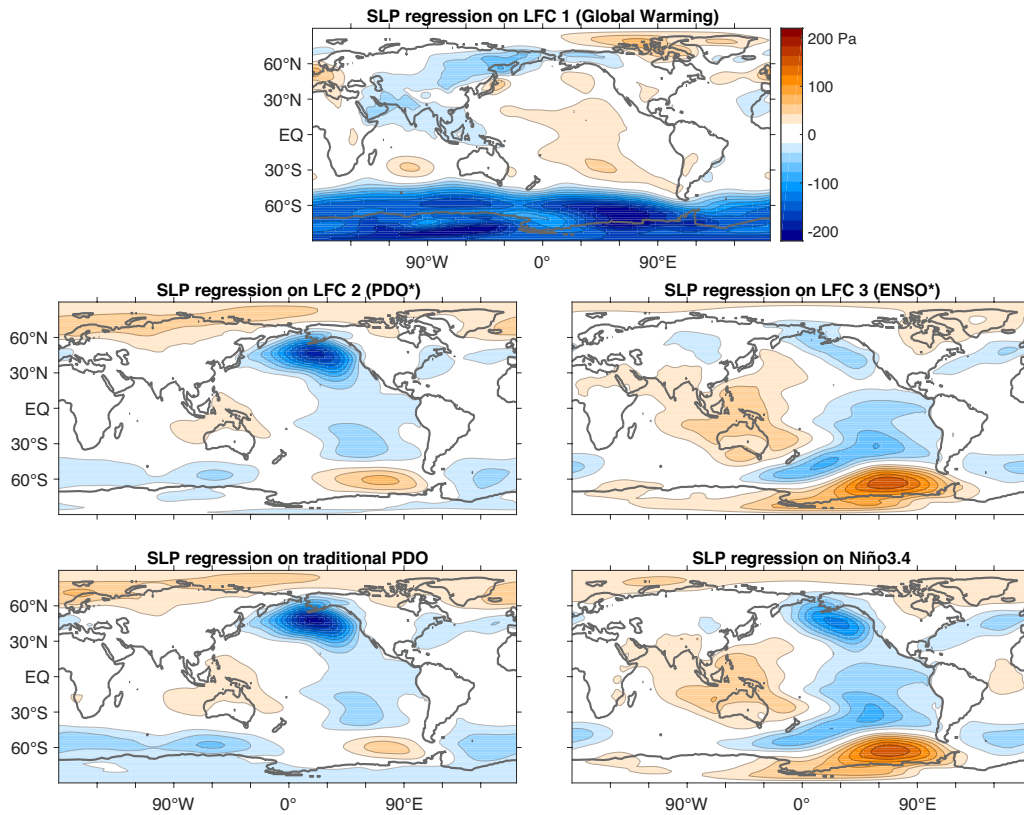


Figure S2. Regressions of 20th Century Reanalysis sea-level pressure (SLP) *Compo et al.* [2011] on the LFCs of monthly Pacific SST anomalies with 3 EOFs retained. The regression of SLP on the traditional PDO index is shown for comparison with LFC 2. The regression of SLP on the Niño3.4 index is shown for comparison with LFC 3. Note the difference in strength of the Aleutian low regression between LFC 3 and Niño3.4.

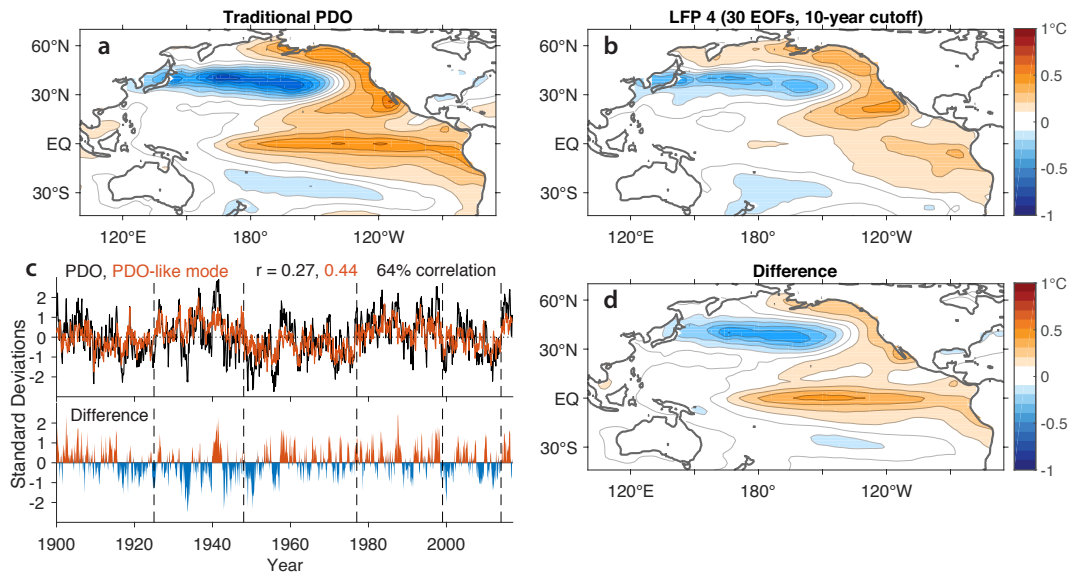


Figure S3. Side-by-side comparison of the traditional PDO and a PDO-like mode obtained through LFCA. (a) The SST pattern associated with the traditional PDO definition [Mantua *et al.*, 1997]. (b) The fourth LFP of Pacific SST (chosen based on its correlation with PDO*), with 30 EOFs retained and optimization of variance remaining after application of a 10-year lowpass filter. (c) Time series of the traditional PDO and the PDO-like LFC 4, rescaled by its 64% correlation with the traditional PDO. The difference between the PDO and the rescaled LFC 4 is shown in the bottom panel of (c) and the SST regression onto this difference is shown in (d).

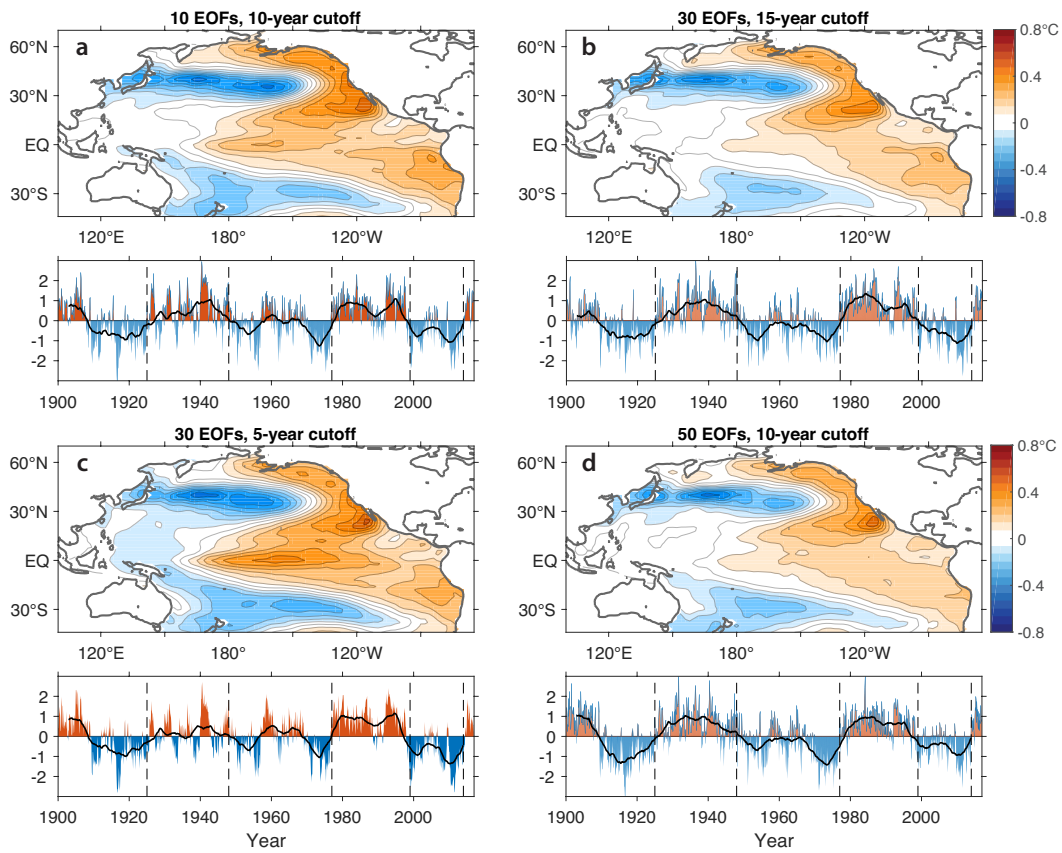


Figure S4. (a)-(d) LFPs and LFCs of the most PDO-like mode at four points in the LFCA parameter space (the parameters are shown in the titles and the points are marked in Fig. 3). Vertical lines indicate years with major PDO transitions. Solid lines show the LFCs filtered with a 6-year running average.

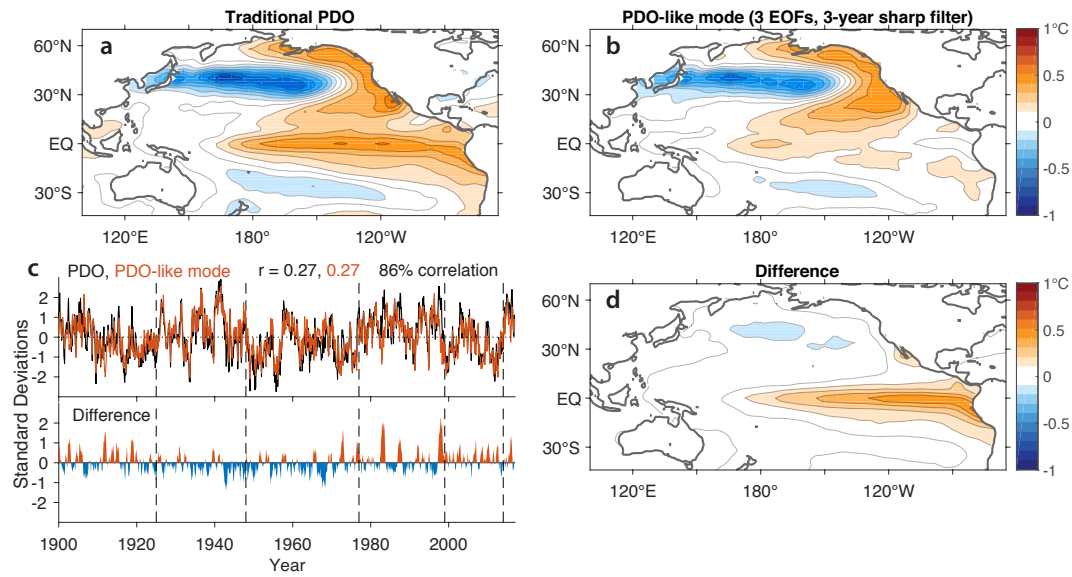


Figure S5. PDO without a connection to tropical SSTs. (a) The SST pattern associated with the traditional PDO definition [Mantua *et al.*, 1997]. (b) PDO-like pattern identified as the second pattern of a spectral discriminant analysis that maximizes the ratio of 3-year to total variance in the leading mode such that this mode has had 3-year timescales filtered out. It looks similar to the traditional PDO, but without the associated variance of tropical Pacific SSTs. The time series (c) of these two PDO-like modes are remarkably similar (86% correlation). Their difference is shown in the bottom panel of (c) and the regression of Pacific SSTs onto their difference is shown in (d). The difference between the traditional PDO and this new PDO-like index is almost entirely in El Niño years, with their differences in SST pattern localized in the eastern equatorial Pacific. This provides a cautionary tale in the interpretation of such SST regression maps; different regions of the SST regression can represent variability at different time scales.

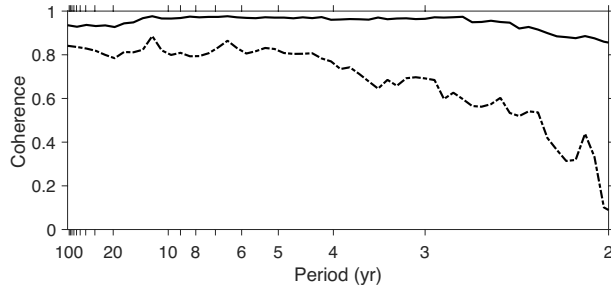


Figure S6. Coherence spectra of PDO* and the traditional PDO index (solid line) and of the PDO-like mode (LFP/LFC 4) of the 30 EOF analysis and the traditional PDO index (dashed line). The coherence spectra are computed using a multi-taper spectral analysis.

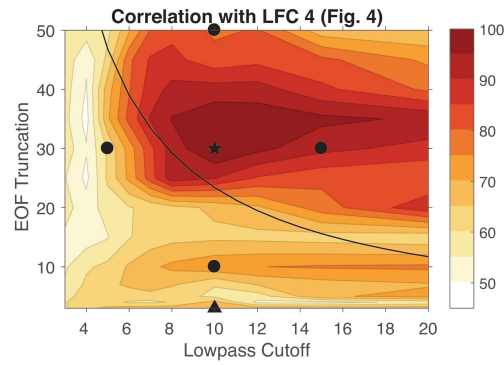


Figure S7. Percent correlation between the mode shown in Fig. 4d (LFC 4, $N = 30$ EOFs, $T = 10$ yr) and the LFC with which it is most correlated at each point in the LFCA parameter space. A black triangle indicates the case shown in Fig. 1, black dots indicate cases shown in Fig. S4, and a black star indicates the case shown in Figs. 4 and S3 (where the correlation is 100% by definition). A black line shows where the dimensionless number (number of years of observations/ T) is equal to $N/2$, at which point the fraction of variance in the PDO-like mode starts to decrease substantially.

References

- Compo, G. P., J. S. Whitaker, P. D. Sardeshmukh, N. Matsui, R. J. Allan, X. Yin, B. E. Gleason, R. S. Vose, G. Rutledge, P. Bessemoulin, et al. (2011), The twentieth century reanalysis project, *Q. J. R. Meteorol. Soc.*, *137*(654), 1–28.
- Mantua, N. J., S. R. Hare, Y. Zhang, J. M. Wallace, and R. C. Francis (1997), A Pacific interdecadal climate oscillation with impacts on salmon production, *Bull. Am. Meteorol. Soc.*, *78*(6), 1069–1079.
- Newman, M., M. A. Alexander, T. R. Ault, K. M. Cobb, C. Deser, E. Di Lorenzo, N. J. Mantua, A. J. Miller, S. Minobe, H. Nakamura, et al. (2016), The Pacific Decadal Oscillation, revisited, *J. Climate*, *29*(12), 4399–4427.